

1.25 Å Resolution Crystal Structures of Human Haemoglobin in the Oxy, Deoxy and Carbonmonoxy Forms

Sam-Yong Park^{1*}, Takeshi Yokoyama¹, Naoya Shibayama²
Yoshitsugu Shiro³ and Jeremy R. H. Tame^{1*}

¹Protein Design Laboratory
Yokohama City University
Suehiro 1-7-29, Tsurumi
Yokohama 230-0045, Japan

²Department of Physiology
Division of Biophysics, Jichi
Medical University, 3311-1
Yakushiji, Shimotsuke
Tochigi 329-0498, Japan

³Biometal Science Laboratory
RIKEN SPring-8 Center
1-1-1 Kouto, Mikazuki, Sayo
Hyogo 679-5148, Japan

The most recent refinement of the crystallographic structure of oxyhaemoglobin (oxyHb) was completed in 1983, and differences between this real-space refined model and later R state models have been interpreted as evidence of crystallisation artefacts, or numerous sub-states. We have refined models of deoxy, oxy and carbonmonoxy Hb to 1.25 Å resolution each, and compare them with other Hb structures. It is shown that the older structures reflect the software used in refinement, and many differences with newer structures are unlikely to be physiologically relevant. The improved accuracy of our models clarifies the disagreement between NMR and X-ray studies of oxyHb, the NMR experiments suggesting a hydrogen bond to exist between the distal histidine and oxygen ligand of both the α and β -subunits. The high-resolution crystal structure also reveals a hydrogen bond in both subunit types, but with subtly different geometry which may explain the very different behaviour when this residue is mutated to glycine in α or β globin. We also propose a new set of relatively fixed residues to act as a frame of reference; this set contains a similar number of atoms to the well-known “BGH” frame yet shows a much smaller rmsd value between R and T state models of HbA.

© 2006 Elsevier Ltd. All rights reserved.

Keywords: X-ray crystallography; nuclear magnetic resonance; NMR; conflict; function

*Corresponding authors

Introduction

When the first X-ray crystal structures of human haemoglobin (Hb) were solved, the structures of the deoxy and aquo-met (Fe^{3+}) protein were found to be distinct. From a comparison between them, Perutz put forward his famous “trigger” hypothesis in which Hb switches between two quaternary states depending on the pull of haem ligands on the proximal histidine.^{1,2} The two quaternary conformations found for deoxy and liganded Hb were

explicitly identified with the tense (T) and relaxed (R) states of the Monod–Wyman–Changeux model of protein cooperativity.³ According to the trigger hypothesis, the low oxygen affinity T state is stabilised by salt bridges on the protein surface, which are broken as the subunits switch tertiary conformation on ligand binding. The model has been subjected to numerous tests and is found to provide an excellent fit to a wide range of experiments, performed on both adult Hb (HbA) and mutant Hbs, leading to the widespread view that Hb is thoroughly understood. The pressing clinical need for a safe, cheap blood substitute, and the search for anti-sickling agents to combat sickle-cell anemia, led to a renaissance in Hb research in the 1990s, however, which produced some surprising results. For example, heterotropic effector molecules such as diphospho-glycerate (DPG) and bezafibrate (BZF) have long been known to lower the oxygen affinity of Hb.^{4,5} This has generally been interpreted in terms of the effectors preferentially (even exclusively) binding to the T state of Hb, and the fall in oxygen affinity

Abbreviations used: HbA, adult human haemoglobin; Mb, myoglobin; COHb, carbonmonoxy haemoglobin; oxyHb, oxy-haemoglobin; DPG, diphospho-glycerate; BZF, bezafibrate; L35, 2-[4-(3,5-dichlorophenylureido)phenoxy]-2-methylpropionic acid; PDB, Protein Data Bank.

E-mail addresses of the corresponding authors:
park@tsurumi.yokohama-cu.ac.jp;
jtame@tsurumi.yokohama-cu.ac.jp

being due to the shift in the allosteric equilibrium. Contrary to this view, kinetic experiments showed that the oxygen affinity of both T and R states are changed significantly by these molecules.⁶ Recent careful examination of oxygen equilibrium curves confirms that the affinity of the R state of Hb falls in the presence of BZF,⁷ and the crystal structure of horse carbonmonoxy Hb (COHb) bound to BZF, or to the related compound 2-[4-(3,5-dichlorophenylureido)phenoxy]-2-methylpropionic acid (L35), is found to be in the R conformation.^{8,9} These results suggest far greater control of oxygen affinity within each quaternary structure than has been generally recognised. There is therefore a need for precise and accurate models of the protein in order to monitor these relatively small tertiary changes, which have profound functional consequences. The trigger hypothesis placed heavy emphasis on the position of the iron atoms relative to the haem plane, yet the changes found on comparing previous structures are comparable to the expected errors in the models refined in the 1980s.

From his 1970 models of deoxy and met-Hb, Perutz predicted that oxygen could not bind to the β subunits in the T state due to severe steric hindrance by the distal valine, Val67 β .¹ In the R state, the valine moves relative to the haem to create space for the ligand; Val62 α is relatively static compared to the α haem. The close contact between bound ligands and the distal residues led to the proposal that steric hindrance is the main effect by which Hb weakens carbon monoxide binding while binding oxygen strongly. It is known from model haem compounds that carbon monoxide tends to bind along the haem normal, whereas oxygen adopts a bent geometry. Since the first report of functional studies of human Hb produced using recombinant DNA, artificial mutants of the protein have played an important role in testing different hypotheses concerning the mechanism of ligand selectivity and control of affinity. A large number of such mutants have been made to test the roles of the distal valine and histidine residues (Val E11 and His E7) in both the α and β subunits.^{10–14} These data have been interpreted using the current model of oxyHb refined by Shaanan in 1983 (PDB 1HHO).¹⁵ This suggests a hydrogen bond between the oxygen ligand in the α subunits, but not in the β subunits, despite the similar architecture of the haem pockets. Replacing the distal histidine of the α subunits (His58 α) with glycine leads to a drop in oxygen affinity and rise in CO affinity, but the equivalent β subunit mutant was very different, and showed little change in oxygen affinity on replacing the distal histidine with glycine.¹² This result fitted very well with the model by Shaanan. More recently, NMR data have shown a hydrogen bond to the ligand does form in both subunits of oxyHb.¹⁶ Re-refinement of oxyHb using the original X-ray data suggests that the protein was in fact largely oxidised to the met form. This is not too surprising, since the data (to 2.1 Å resolution) were collected using X-ray film and a rotating anode generator from crystals

mounted in capillaries and cooled to 4 °C. The oxy complex is sensitive to X radiation and, without cryo-cooling, long exposure to X-rays will inevitably lead to oxidation. Shaanan did not have cryo-cooling or advanced refinement methods at his disposal 23 years ago, and we are therefore in a significantly better position to handle all steps in the structure determination process once a crystal has been obtained.

The chemical stability of COHb has made carbon monoxide a ligand of choice for studying the R state, and the majority of liganded Hb structures in the PDB are in the CO form. The earliest crystal structure of COHbA was refined to 2.7 Å, at which resolution it was necessary to enforce planar haem groups and a straight, perpendicular Fe-C-O geometry in order to limit the number of parameters refined.¹⁷ A later model to 2.1 Å resolution allowed the ligand to be given some freedom, and suggested small deviations from the haem normal.¹⁸ Even in 1990, the data were collected for this refinement using a Xentronics area detector and a fixed anode X-ray generator, leading to poor data quality by today's standards. Other crystal structures have suggested a much more bent ligand geometry. Refining COMb to 1.5 Å in 1986, Kuriyan and colleagues found an Fe-C-O angle of around 150°. ¹⁹ A similar angle was found in COHb refined to 2.2 Å using human Hb, which transpired to be a mutant at the surface.²⁰ Spectroscopic studies have not supported the idea of a bent geometry, and strongly suggest the ligand pushes the distal residues aside to adopt its preferred conformation. One difficulty with the crystallographic refinements is that the ligand oxygen atom is largely unconstrained by its one chemical bond, and in the absence of very high resolution data the model must be restrained carefully using prior information. The introduction of maximum likelihood refinement has greatly reduced the bias of models, but there is still no substitute for very high-resolution data of high quality.

The highest resolution structure of deoxy HbA in the PDB at present is that of Fermi and colleagues, refined to 1.74 Å using real space refinement in 1984.²¹ The structure of this crystal form was solved again to 1.8 Å using a crystal cryo-cooled to 120K.²² Here we describe the crystal structure of deoxyHbA at room temperature, refined to 1.25 Å. We have also obtained 1.25 Å data from single cryo-cooled crystals of oxyHb and COHb in order to refine the structures with minimal restraints on the ligand. These three models have been refined with anisotropic displacement parameters using SHELX,²³ giving the most accurate models of human Hb to date, and allowing us to observe unambiguously the nature of the interactions of oxygen with the protein in electron density maps.

Results

Each of the three models was refined using known Hb structures as starting models, refinement pro-

ceeding smoothly to give the final statistics shown in Table 1. The overall structure of each model closely matches previous Hb structures, and differences are largely confined to rotamer errors, water structure and a general improvement in model geometry. Comparing our deoxy tetramer model with 2HHB, we find 22 side-chains with different rotamers, 12 of these being leucine. There are also 31 different rotamers in the COHb model compared to 1HHO, which has a pep-flip error at Ala71 α . It has been suggested that this pep-flip is diagnostic of the R state.²⁴ The three models described here (deoxy Hb at room temperature and cryo-cooled oxyHb and COHb), and the earlier model of deoxyHb at 120K (PDB 1A3N), were compared using ESCET²⁵ to find regions of invariant structure within the $\alpha\beta$ dimer. A core set of 74 C α atoms was found, 26.3% of the total, which define a relatively fixed frame: α 23–42, 57–63, 101–111, 118–125 and β 51–57, 110–116, 119–132. This set of residues shows some similarity to the widely used “BGH frame” de-

scribed by Baldwin & Chothia,²⁶ but differs in key respects. It comprises the end of the G helix and start of the H helix in both subunits, plus the B and C helices and central E helix from the α chain. Surprisingly, it also includes the DE corner of the β chain. The α chain contributes more residues, in keeping with its relatively invariant structure on ligand binding, and its E helix seems more rigidly held than the β chain B helix. Using the 74 selected C α atoms, the rmsd value between the oxy and deoxy structures described here is 0.20 Å. For the 78 C α atoms of the BGH frame, the rmsd value is 0.46 Å. Comparing the oxyHb model with the cryo-cooled deoxyHb structure (PDB 1A3N) gives rmsd values of 0.17 Å and 0.50 Å with the new frame and BGH frame, respectively. The results with high resolution human Hb mirror those found earlier with tuna Hb,²⁷ and it is hoped this frame may assist comparative studies of human and animal Hbs.

Liganded models

Comparing the oxyHb model with PDB 1HHO, the rms deviation among main-chain atoms is 0.67 Å, and the maximum atom displacement is >7 Å. The largest movements are found at the C terminus of the α chain, which was not well ordered in the real-space refinement by Shaanan. Significant differences are also found at the β chain N terminus. More important changes are found within the haem pockets, where the oxygen molecule is clearly visible in the high-resolution electron density maps (Figure 1). It can be seen that the distal histidine is in a position to hydrogen bond to the ligand in both the α and β subunits, a clear contrast to PDB 1HHO where no such bond was seen in the β subunits. The existence of such a hydrogen bond was first proposed in 1974, on the basis of EPR measurements,²⁸ and confirmed by crystallography nine years later. Since mutation of the distal histidine to glycine greatly weakens oxygen binding to α globin but not β globin, it appears that the hydrogen bond made by His E7 β is much weaker than that made by His E7 α .¹² The geometry of the ligand and distal histidine is slightly different in the two subunits, with the O2 atom lying 2.7 (\pm 0.1) Å from the N ϵ atom of the distal histidine in the α subunits, and 3.0 Å away in the β subunits. The high resolution model therefore confirms the presence of the hydrogen bond in both subunits found by NMR.¹⁶ It is interesting to note that the O1 atom, directly bonded to the haem iron, lies 2.8 Å from the N ϵ atom in the α subunits, but 3.1 Å away in the β subunits. The electron density is also suggestive of a weaker hydrogen bond in the β subunits, having a lower level around the O2 atom (Figure 1). This suggests that both oxygen atoms may hydrogen bond to the histidine, but the more distant imidazole group of the β subunits is apparently unable to bind strongly to the ligand. The distal histidine is also marginally closer to bound CO in the α subunits,

Table 1. Crystal parameters, data collection and structure refinement

	DeoxyHbA	OxyHbA	CO-HbA
<i>A. Crystal data</i>			
Resolution range (Å)	25.0–1.25	25.0–1.25	25.0–1.25
Space group	<i>P</i> 2 ₁	<i>P</i> 4 ₁ 2 ₁ 2	<i>P</i> 4 ₁ 2 ₁ 2
Cell parameters (Å, °)	<i>a</i> =63.1, <i>b</i> =82.9, <i>c</i> =53.6, β =99.3	<i>a</i> = <i>b</i> =53.4, <i>c</i> =191.7	<i>a</i> = <i>b</i> =53.3, <i>c</i> =189.8
Reflections (Measured/Unique)	398,793/ 145,478	299,269/ 73,528	581,378/ 76,777
Completeness (%, overall/outer shell)	97.0/93.8	94.2/81.3	100.0/ 100.0
Mean $\langle I \rangle / \langle \sigma(I) \rangle$	6.3	22.5	5.8
Multiplicity	2.7	4.1	7.6
<i>R</i> _{merge} (%) ^a (overall/outer shell)	6.7/46.5	5.3/27.7	6.1/53.3
<i>B. Refinement statistics</i>			
Resolution range (Å)	20.0–1.25 14.7	20.0–1.25 19.2	20.0–1.25 17.9
<i>R</i> -factor (%) ^b	(<i>F</i> _o >4 σ , 97,606) 17.9 (<i>F</i> _o >0 σ , 145,396)	(<i>F</i> _o >4 σ , 68,554) 19.5 (<i>F</i> _o >0 σ , 73,491)	(<i>F</i> _o >4 σ , 67,451) 18.3 (<i>F</i> _o >0 σ , 76,575)
Solvent molecules	221	228	212
<i>C. rms deviations from ideal</i>			
Bond length (Å)	0.012	0.011	0.020
Bond angles (°)	0.030	0.027	0.028
Chiral volume (Å ³)	0.060	0.067	0.054
<i>D. Ramachandran plot</i>			
Residues in most favourable region (%)	94.2	93.9	94.0
Residues in additional allowed region (%)	5.8	6.1	6.0

The outer shell has resolution limits of 1.32 Å –1.25 Å.

^a $R_{\text{merge}} = \sum |I_i - \langle I_i \rangle| / \sum I_i$, where I_i is the intensity of an observation and $\langle I_i \rangle$ is the mean value for that reflection and the summations are over all reflections.

^b $R\text{-factor} = \sum_h \|F_o(h) - |F_c(h)|\| / \sum_h F_o(h)$, where F_o and F_c are the observed and calculated structure factor amplitudes, respectively.

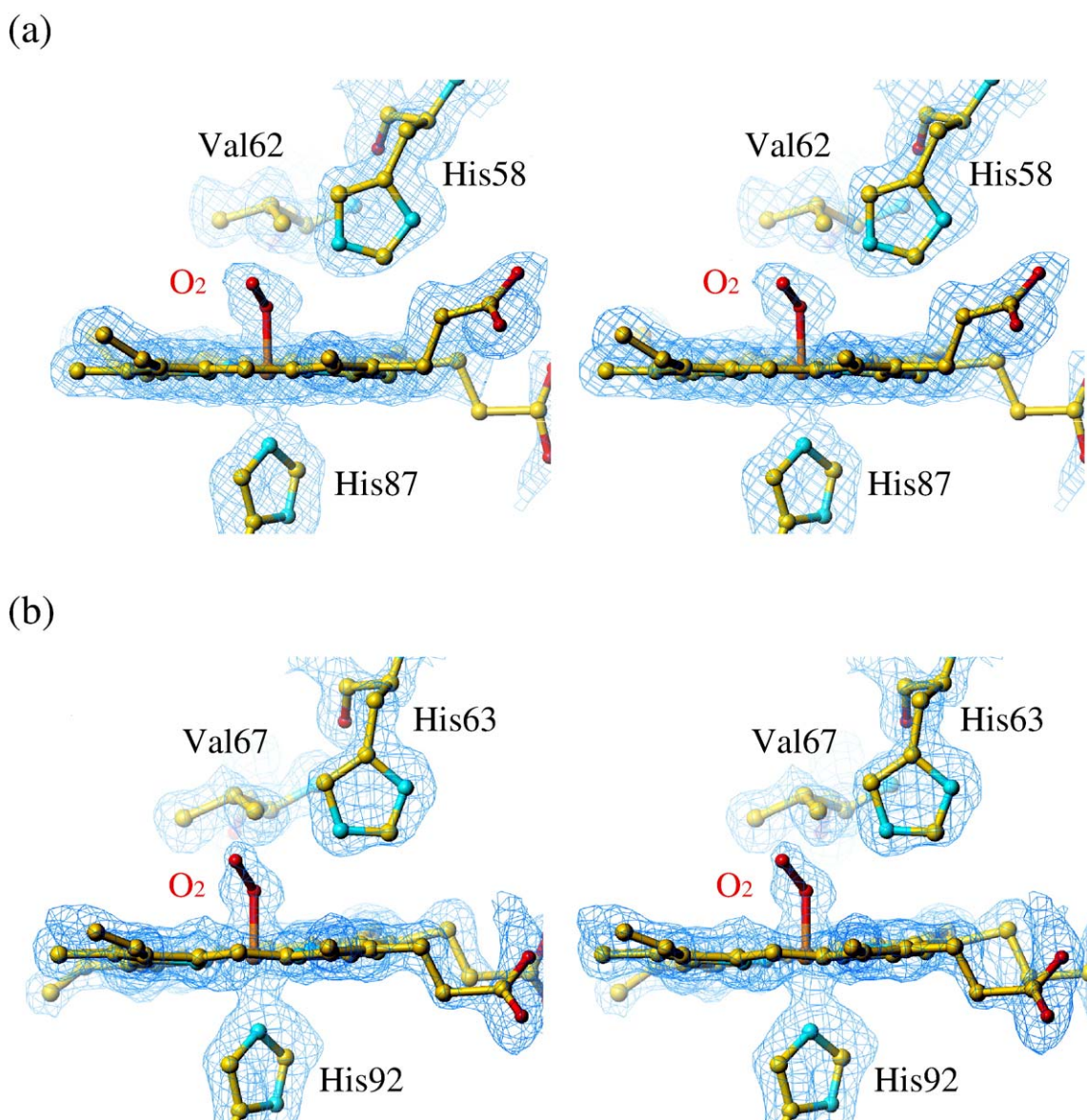


Figure 1. Stereo view of the final $2mF_o-DF_c$ electron density map for oxyHbA, showing (a) the ligand at the α haem and (b) the β chain. In the α subunit, a small peak of density (roughly 1.5σ) is found about 2.2 \AA from the oxygen ligand and 3.1 \AA from Leu29. Leu29 shows some sign of adopting more than one rotamer, which may allow a partially occupied water molecule into the haem pocket. Density is contoured at 1.5σ . It can be seen that the O2 atom of the ligand, not directly bonded to the haem, is better defined in the α pocket than in the β haem pocket density. The lower electron density in the β subunits is indicative of a weaker bond to the distal histidine and greater rotation about the Fe–O bond. Temperature factors for the O2 atoms are similar (35 \AA^2 and 33 \AA^2 in the α and β subunits, respectively).

which may increase discrimination against this ligand (Figure 2). Other minor differences between the oxy and CO structures include the rotamer of Leu83 α , which sits next to the proximal histidine, and a vinyl group on the β haem. Neither difference has an obvious role in the control of ligand affinity. Despite the extensive research devoted to the mechanisms of ligand discrimination by haem proteins, no firm consensus has yet emerged. In the case of Mb, a very high resolution X-ray structure was offered as evidence that all haem proteins discriminate against CO binding in favour of oxygen through purely steric selection,²⁹ but not a single paper was cited from the many on

functional studies of site-directed Mb and Hb mutants. A more recent analysis of the structure by combined quantum and molecular mechanics suggests that steric effects are in fact unhelpful, and ligand discrimination occurs purely through electrostatic effects including hydrogen bond formation.³⁰ OxyHb provides a useful test case for such hypotheses since the α and β subunits show markedly different behaviour. In our model of oxyHb, the Fe–O–O angle is 124° and 126° in the α and β subunits, respectively. The Fe–C–O angles in our model of COHb are 172° and 169° , in good agreement with earlier spectroscopic analyses, and the near-atomic resolution structures of oxy and

carbonmonoxy myoglobin refined by Schlichting and colleagues.³¹ These angles in our models must have an error approaching 3°, however, and are not significantly different in the α and β subunits.

A marked difference is found between the oxyHb and COHb models at Trp14 α . This is because in the oxy model, the tryptophan has a flipped rotamer and points to the outside of the protein. In place of its side-chain, two round, flattened peaks of density are found, which are apparently due to two toluene molecules. Crystallisation of R state Hb using the protocol described by Perutz³² requires one or more drops of toluene be added to the tube. It is unclear why the toluene is not observed in the COHb structure, but this may reflect the different temperature at which the crystals were grown.

Deoxy model

The deoxyHb model presented here is an unusually high resolution structure for a protein the size of Hb (4556 non-hydrogen protein atoms), especially considering that a capillary mounted crystal held at 20 °C was used. The method used is therefore almost identical to that by Fermi and colleagues, who refined the 1.74 Å deoxyHbA structure (PDB 2HHB),²¹ except that a CCD X-ray detector and modern data analysis software were used. In contrast, the 1.8 Å structure (PDB 1A3N) was refined using a cryo-cooled crystal.²² As mentioned above, the main differences between these models are rotamer flips. There are 11 rotamer flips between the deoxy model and 1A3N, generally surface residues close to crystal contacts. PDB 1A3N shows concerted side-chain movements at Glu22 and His117 in the B (β_1) chain, breaking the salt bridge found in the room temperature structures, though the electron density suggests this bond is never strong. None of the three models has this salt bridge in the NCS related D (β_2) chain. The N termini of the β chains are disordered in 1A3N, so that Val1 β and the side chain of His 2 β beyond the C β atom were not modelled. The deoxy model and 2HHB differ only slightly over these residues, which are present in the electron density map but with high temperature factors. A fully occupied water molecule is found in both α subunit haem pockets, hydrogen-bonded to the distal histidine, but there is no trace of a water molecule in the β haem pocket (Figure 3).

The high resolution refinement of deoxyHbA allows us to test the hypothesis of Juers & Matthews^{33,34} that cryo-cooling protein crystals is prone to introduce artefactual hydrogen bonds between long side-chains at protein interfaces. It has been suggested that “for entropic reasons such side-chains, as well as surface solvent molecules, tend to be somewhat disordered at room temperature but can form extensive hydrogen-bonded networks on cooling.” The reasoning is that side-chain entropy must be reduced by two-thirds on cooling from 300K to 100K. Thus Juers & Matthews³³ suggest the 0.6 kcal/mol estimated entropy cost ($T\Delta S$) of restricting rotation about a single bond at

298K will be 0.2 kcal/mol at 100K, making it easier for long side-chains to form hydrogen bonds. However, it is readily seen from the van't Hoff equation³⁵ that any change in equilibrium of any system on changing temperature is primarily an enthalpic, rather than entropic, effect:

$$\frac{d}{dT}(\ln K) = \frac{\Delta H}{RT^2}$$

Salt bridge formation on lowering temperature may therefore have little to do with entropy. Entropy effects arise through changes in the heat capacity change, ΔC_p , and changes in the entropy with temperature follow the equation:

$$S_{T2} - S_{T1} = \int_{T1}^{T2} \frac{C_p}{T} dT$$

In the case of hydrophobic molecules dissolving in water, for example, the process is entropically unfavourable at room temperature, but much less so in boiling water, when the dissolution of such compounds becomes enthalpically disfavoured. In this case the contribution of the entropy change to the overall ΔG value is much smaller at higher temperature.³⁶ The $T\Delta S$ term is not simply proportional to absolute temperature, since entropy is itself a function of T , and the appearance of hydrogen bonds and salt bridges on cryo-cooling cannot be ascribed to entropy simply from an examination of static models. Since charged side-chains release water molecules on salt bridge formation, the overall entropy change need not be negative, and need not have the same sign at high and low temperatures. From the perspective of these released solvent molecules, salt bridge formation will be favoured at higher temperatures, and indeed surface salt bridges are commonly found in thermostable proteins.³⁷ Differences at protein surfaces may arise due to the addition of dehydrating cryo-protectants, and it is well-known that oxyHb can be slowly converted to deoxyHb merely by the addition of high concentrations of PEG.³⁸ In the case where no allosteric change is involved and charged side-chains are in rapid equilibrium between free and salt-bridged conformations, even a very brief soak in cryo-protectant may be enough to change that equilibrium on a very short time-scale. The interesting differences found by the Matthews group between room temperature and cryo-cooled crystals are not therefore necessarily due to entropic differences. Overall we find no evidence in the cryo-cooled structure of surface salt bridges not found in the 20 °C model, and the key salt bridges stabilising the T state are present in both models.

Fitting a least-squares plane to the 24 inner atoms of each haem (apart from the iron atom), the distance of the iron from the plane can be measured. The results are shown in Table 2. In agreement with the mechanism described by Perutz, the iron atom moves significantly into the haem plane on ligation, but a little less in the case of oxygen than carbon

monoxide. For the 24 non-iron atoms, the maximum deviation from the best-fit plane is in the range 0.2 Å–0.3 Å in each case, and in each model the β haem shows the greatest deviation. If only the four nitrogen atoms are considered, then the displacements for the deoxy and oxy structures decrease, and those for COHb increase. Using the four-nitrogen plane, Fe displacements in deoxyHb range from 0.3 Å–0.4 Å. While the movement of the iron atoms is functionally significant, it is clearly a small fraction of a chemical bond length.

Discussion

A wide array of studies of mutant, chemically modified or lattice-constrained Hb models have largely supported Perutz's two-state characterisa-

tion of Hb, but greatly expanded the definitions of these states. The extensive studies by Paoli and colleagues have shown how T state Hb responds to increasing ligation, and how Hb is constrained by the crystal lattice.^{39,40} These lattice forces, and the nature of the precipitating agents used to grow protein crystals, have led to considerable debate concerning the structure of liganded Hb, and whether or not the canonical R state embodied by the 1983 refinement of oxyHb (PDB 1HHO),¹⁵ is in fact an artefact of crystallisation. It has been strongly argued that the "high salt" conditions used may have artificially stabilised the observed conformation, and the R2 form found by Silva and co-workers using PEG-grown Hb crystals at pH 5.8 may be more relevant to the protein in solution.^{24,41,42} This view gained such currency that it was stated as fact, without qualification or supporting citation, by Xu

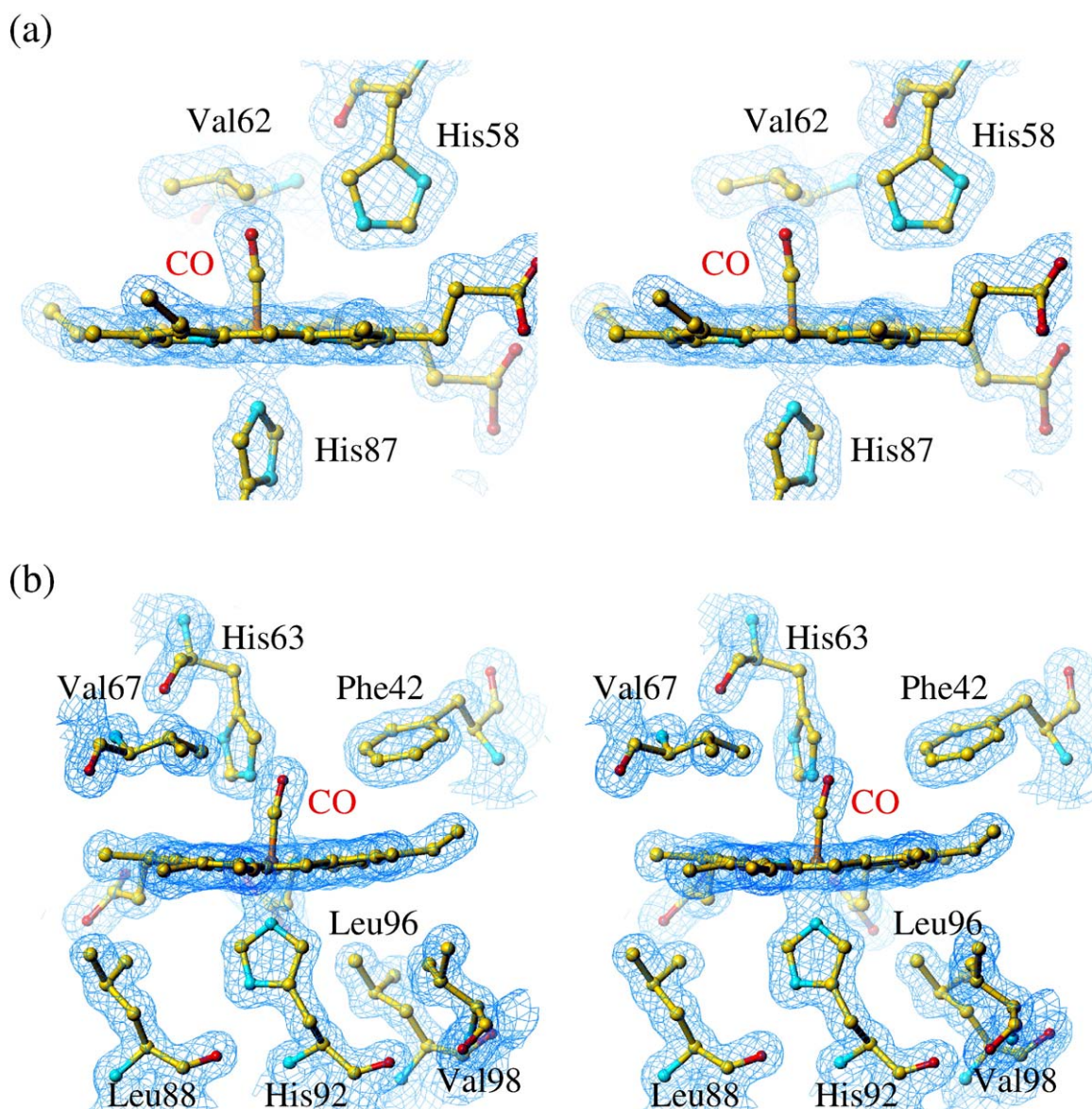


Figure 2. Stereo view of the final $2mF_o-DF_c$ electron density map for COHb, showing (a) the α haem and (b) the β haem. Density is contoured at 1.5σ . The C termini of the α and β subunits are shown in (c) and (d), respectively. Tyr141 α and Tyr145 β show substantial shifts compared to PDB 1HHO.

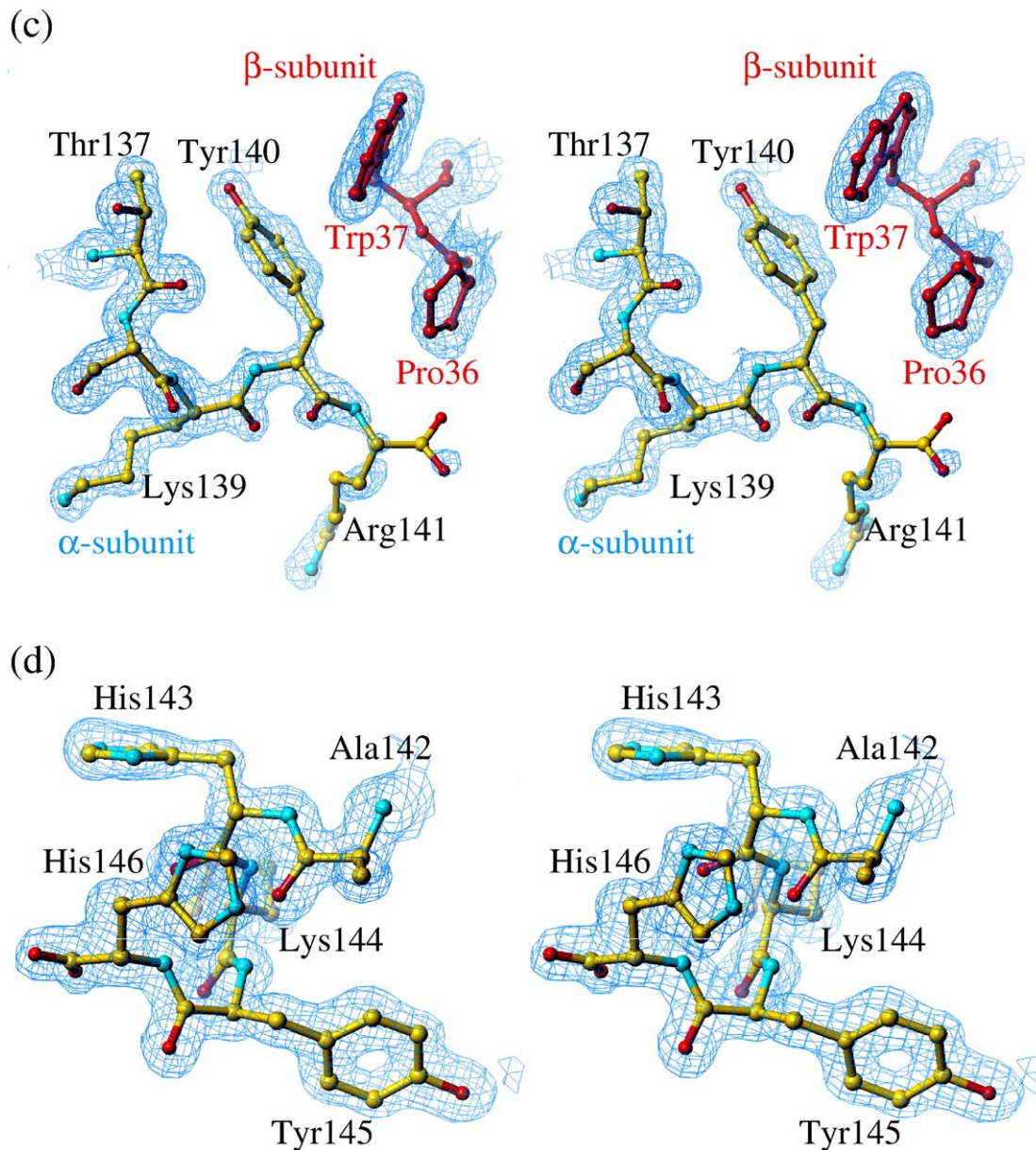


Figure 2 (legend on previous page)

and colleagues.⁴³ Given the decidedly non-physiological pH at which crystals of the R2 structures were grown, others have suggested this form is of little relevance to oxygen transport within the body.⁴⁴ The recent use of dipolar couplings to determine the dimer–dimer rotation in COHb with isotopically labelled protein suggests that the high salt R state structure is indeed as close to the solution structure as the R2 structure,^{45,46} in agreement with the view⁴⁷ that the high salt structure cannot be dismissed as a crystallographic anomaly. In fact the high-salt model used (PDB 1IRD) was our earlier unpublished COHb structure that has two rotamer errors, at Gln β 39 and His β 77, corrected in the new model (PDB, 2DN3) described here, which presumably agrees even better with the NMR data. Nevertheless, the NMR data showed substantially

better agreement with PDB 1IRD than the oxyHbA model by Shaanan, demonstrating that high resolution X-ray data are important when comparing data from the two biophysical techniques. This is further shown by NMR experiments on deoxyHbA,⁴⁸ which gave better agreement with PDB 1A3N²² than 2HHB due to the rotamer error in the latter model at His103 α . The use of 1HHO and 2HHB as “canonical” models against which others are compared is therefore clearly a dangerous practice prone to give spurious differences.

The use of the terms R and T state underlies much of the debate on Hb. In our view, each quaternary structure, R and T, represents a significant volume (rather than a point) in conformational space. Often the terms “R state” and “R2 state” are used to indicate particular models in PDB, and this has led

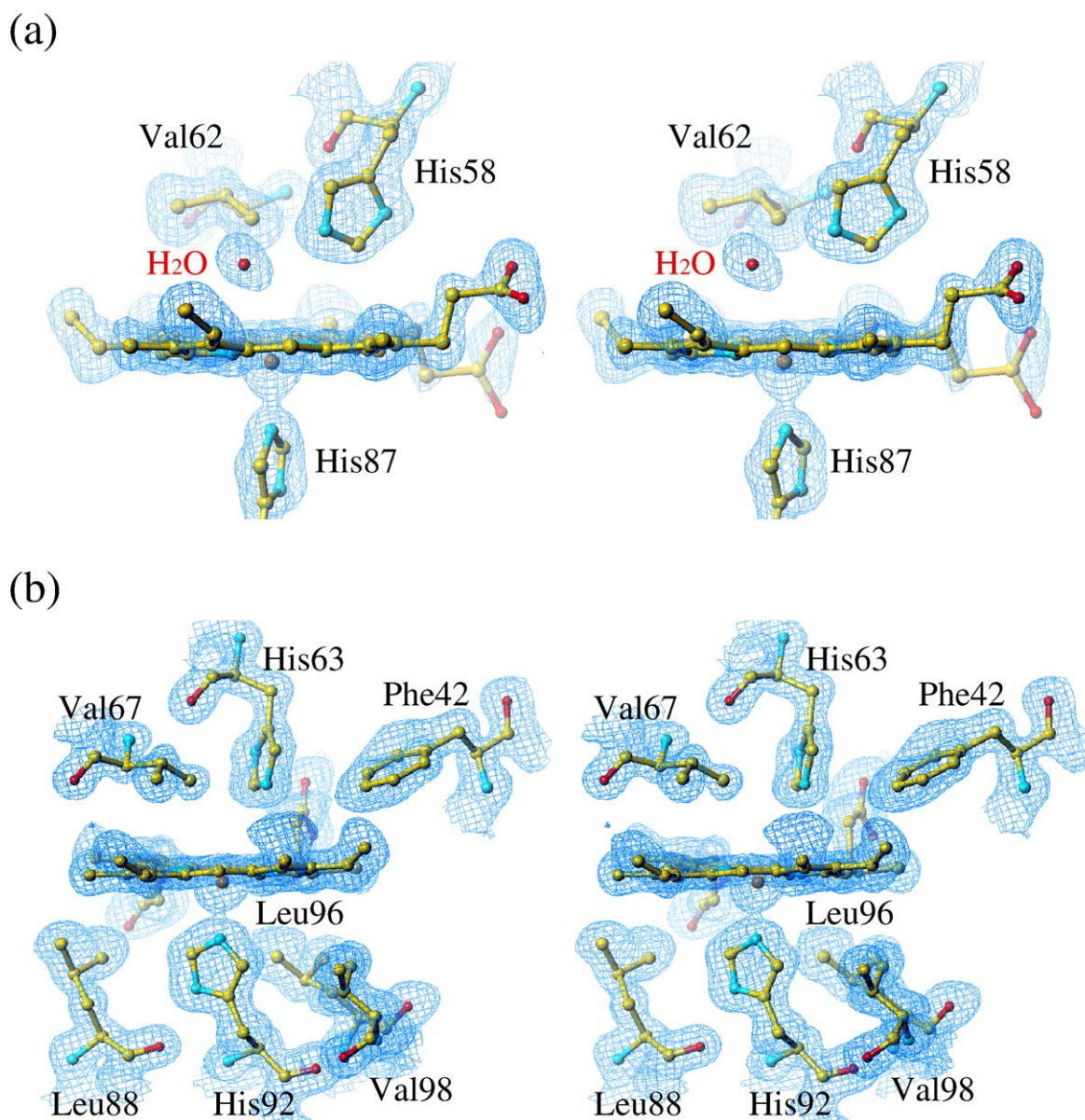


Figure 3. Stereo view of the final $2mF_o-DF_c$ electron density map for the haem pockets of deoxyHb, (a) the α subunit and (b) the β subunit. Density is contoured at 1.5σ . The α subunits have fully occupied water molecules present, and the β subunits have none, in agreement with previous structures.

Kavanaugh and colleagues to choose to label the structure of liganded Hb in solution the “R^e” ensemble.⁴⁹ Since the R state was originally conceived as a thermodynamic state, we prefer to use the name in this sense,³ rather than to indicate a particular structure in the PDB. Likewise, the deoxy

Table 2. Distance of Fe from the least squares haem plane (Å)

	Deoxy	CO	Oxy
α	0.50 0.60	0.01	0.09
β	0.45 0.40	0.01	0.06

The distances shown were calculated using a plane fitted to the 24 inner non-iron atoms of the haem.

form of Hb appears capable of significant conformational flexibility, and the “T state” encompasses a variety of forms.^{27,39,40,49–55} We prefer to use interactions within a particular Hb model to define its quaternary state (Table 3), rather than dimer rotation angles or structural overlays with “canonical” (and 20 year old) models from the PDB. This is in keeping with the use of spectroscopic “markers” to define quaternary state, these arising from interactions made by Tyr42 α , Asp94 α , Trp37 β and the haems.⁵⁶

There is clearly scope for confusion where new and old definitions are mixed. Recently Gong and colleagues⁵⁷ described NMR measurements indicating that allosteric effectors cause ligated Hb to move away from the R2 form toward the R form. This they

Table 3. Side-chain hydrogen bonds characteristic of the T and R states

Residues	COHb	OxyHb	DeoxyHb
Lys40 α_1 -His146 β_2	-	-	2.83 (2.59) ^a
Tyr42 α_1 -Asp99 β_2	-	-	2.51 (2.52)
Asp94 α_1 -Trp37 β_2	3.67	3.68	2.85 (2.84)
Asp94 α_1 -Asn102 β_2	2.74	2.83	- (-)
Arg141 α_1 -Asp126 α_2	-	-	2.78 (2.66)
Asp94 β_1 -His146 β_1	-	-	2.60 (2.84) ^a
Trp37 β_1 -Asn102 β_1	2.95	2.90	- (-)

All distances are shown in Ångstrom units. The expected error is of the order of 0.1 Å, and distances are shown to one extra decimal place. The deoxy structure has a tetramer in the asymmetric unit, and the distance for the non-crystallographic symmetry equivalent bond is shown in brackets. A hyphen indicates no hydrogen bond is formed between the two atoms.

^a The two equivalent distances in the asymmetric unit are larger than the expected error in the position of a non-hydrogen atom.

describe as a “quaternary structure change”, and they criticise the “global” allosteric model of Yonetani⁵⁸ on this basis. The disagreement is rather linguistic, since the global allosteric model simply acknowledges, quite correctly, that allosteric effectors may depress oxygen affinity strongly without switching Hb to the T state. This has been described traditionally as an absence of quaternary change. Gong and colleagues also suggest there is “no direct information that deoxyHbs exhibit multiple T types of structure”, contrary to a number of reports cited above, but this may reflect the definitions they apparently use for the terms R and T state. $\alpha\beta$ dimer rotation angles are perhaps too insensitive a test to discern differences within the T state, even though haem-haem interaction is clearly apparent in T state crystal structures.³⁹

The belief that each crystal model represents a distinct thermodynamic state has naturally led crystallographers to interpret new Hb structures as intermediates on the allosteric transition pathway. Thus, the R2 model was first suggested to be an intermediate,⁴¹ and later the true end-point of the transition.²⁴ In 2002, Safo and colleagues refined to 2.16 Å the structure of COHbA at pH 6.4,⁵⁹ and suggested their model too is an intermediate on the allosteric transition, since the hydrogen bond between Thr38 α_1 and His97 β_2 found in earlier structures of R state HbA is missing. Our 1.25 Å models of oxyHb and COHbA also lack this hydrogen bond, and we believe the threonine conformation in the older models is probably a rotamer error. We see no reason to interpret the minor changes between these models in terms of allosteric intermediates, but view the models rather as points in the volume of conformational space labelled “R state”. There is no evidence that these slightly different models represent R \leftrightarrow T intermediates, other than changes from 1HHO. Indeed, by growing crystals at very low pH, it cannot be certain that the final model does not represent an intermediate on the acid unfolding pathway. A number of

crystal structures of Hb in which the protein is chemically or physically restrained have been solved,^{60,61} and these are more likely to represent intermediate forms than crystals of unmodified fully liganded Hb grown from novel conditions. The latter will more probably yield models simply sampling the conformational space of the unrestrained protein. Safo and colleagues have published a number of structures of liganded HbA, and suggest the existence of R, RR2, R2 and R3 forms of the protein.⁶² As noted above, we feel it is unhelpful to label PDB 1HHO “the R state”, and we do not assume that minor differences from this model must be physiologically relevant. Many of these differences clearly arise from the very different crystallographic procedures used today and 20 years ago. From a thermodynamic point of view, these new structures may be considered individual points within “R-state space”, sampled by crystallising the protein under slightly different conditions. While the new structures have expanded appreciation of the conformational flexibility of liganded Hb, their interpretation and significance remains a matter of debate.

It is worth stressing that the oxygen affinity of the T and R states is not fixed, but dependent on solution conditions. This has been realised for the T state for many years,⁶³ but only in the last four years has it been discovered that heterotropic ligands can strongly suppress oxygen binding by binding to the R state, without blocking the haem pocket or preventing movement of the haem iron atom.^{8,9,58,64} This discovery overturns a principal assumption underlying much Hb research of earlier decades. Further analysis is required to understand the mechanism, but the lack of atomic shifts on binding these effector molecules (even at very high resolution) implies that a dynamical change is involved, which cannot be seen in static models. The high resolution models described here provide much more accurate and precise details of the interactions formed between Hb and its ligands oxygen and carbon monoxide, and offer a more reliable framework with which results from other biophysical experiments can be interpreted. In particular, the high resolution model of oxyHb presented here explains both the detection by NMR of hydrogen bonds between ligand and distal histidine, and the very different functional result of mutating that histidine to glycine in the α and β subunits.

Materials and Methods

Protein preparation, crystallisation and data collection

HbA was prepared as described, and crystals of deoxy, oxy and carbonmonoxy HbA were grown using standard protocols.³² Deoxy crystals were grown at pH 6.5, at 20 °C, under an atmosphere of nitrogen. OxyHb crystals were grown from 10 mg/ml oxyHb solutions containing 2.4 M

sodium/potassium phosphate (pH 6.7), 10%(v/v) glycerol and 2%(v/v) toluene at 4 °C. Tetragonal crystals formed within three days. COHb crystals were grown using the batch method from solutions containing 2.4 M sodium/potassium phosphate (pH 6.7), 10% glycerol at pH 6.7 and 20 mg/ml carbonmonoxy Hb at 20 °C under an atmosphere of carbon monoxide. Both deoxyHb and COHb diffraction data were obtained using synchrotron radiation at RIKEN beam line BL44B2 (RIKEN Structural Biology Beamline II) of SPring-8, Harima, Japan. The COHb crystals were flash-cooled to 100K in mother liquor containing 25% glycerol. The deoxy crystal was mounted in a capillary under nitrogen, and held at 20 °C throughout data collection. Intensity data were collected with a MAR CCD detector. The wavelength of the incident X-rays was 0.7 Å. COHb diffraction data were integrated and scaled with MOSFLM⁶⁵ and SCALA, part of the CCP4 package.⁶⁶ DeoxyHb data sets were integrated, merged and scaled with HKL2000 and SCALEPACK.⁶⁷ X-ray diffraction from oxyHb crystals was measured using an R-AXIS-V image plate detector at RIKEN beamline BL45XU at SPring8. The oxy crystal, cryo-cooled to 100K, was mounted with the *c* axis close to the axis of rotation, and three data sets were collected with different distances to the image plate (200 mm for high, 360 mm for medium and 620 mm for low resolution data). The wavelength of the incident X-rays was 1.0 Å. These data sets were integrated, merged and scaled with HKL2000 and SCALEPACK.⁶⁷ In the case of oxyHb, the degree of oxidation after data collection was estimated by dissolving the crystal and observing the spectroscopic change on the addition of cyanide ions. This suggests that no more than 7% of the haems were oxidised at the end of data collection.

Structure refinement

The structures of human COHb¹⁷ and deoxyHb²² reported previously were used as starting models for the refinement of CO and deoxy high resolution structures with the program X-PLOR v.3.851,⁶⁸ with the CO ligand and solvent molecules omitted, and the partly refined model of COHb was used as a starting model for the oxy structure. Several steps of simulated slow-cool annealing were performed, followed by model rebuilding using the graphics program TURBO-FRODO.⁶⁹ The slow-cool protocol ($T=3000$ K) was used to calculate unbiased omit maps. In the case of COHb, after inclusion of 182 solvent molecules and refining isotropic temperature factors, the *R*-factor was 21.7% and free *R*-factor (using 5% of measured reflections) was 24.4% for data between 20.0 Å and 1.25 Å. For the oxy structure the *R*-factor was 23.9% and free *R*-factor 25.7% at this stage. The CO and oxy ligands were then modelled into the electron density maps and refinement continued with SHELXL. Two toluene molecules were located within oxyHb in a hydrophobic pocket in the α -subunit, but no restraints were applied to maintain their expected geometry. Anisotropic temperature factors were calculated for all atoms except the haem and CO ligand. The F_o-F_c difference electron density map revealed a strong ring around the iron atom in the haem plane, clearly suggesting anisotropy of the thermal motion of the iron atom. All atoms of the haem and CO ligand were modelled anisotropically from this point on. Solvent molecules were placed automatically by SHELXL. The deoxy, oxy and carbonmonoxy models were refined to free *R* factors of 16.4%, 18.3% and 16.3% with 241, 283 and 325 water molecules per asymmetric unit, respectively. The water structure was then pruned by removing any which

did not appear above 2.0σ in the $2F_o-F_c$ map or appear to form hydrogen bonds, before several rounds of refinement using all data. No hydrogen atoms are visible in the final maps. Crystallographic and refinement data are summarised in Table 1. The N-terminal residues are missing from the oxyHb model, and the C-terminal carboxyl group of the α chain in the COHb model is poorly defined. Analysis of the models was carried out with the molecular graphics program COOT.⁷⁰

Protein Data Bank accession codes

Models and X-ray data have been deposited in the RCSB PDB with codes 2DN1 (oxyHb), 2DN2 (deoxy Hb) and 2DN3 (COHb).

Acknowledgements

We thank Dr Shin-ichi Adachi for help with data collection. S.Y.P. is supported by the ISS applied research partnership program. J.R.H.T. also thanks the Japanese Society for the Promotion of Science for financial support.

References

1. Perutz, M. F. (1970). Stereochemistry of cooperative effects in haemoglobin. *Nature*, **228**, 726–739.
2. Perutz, M. F. (1972). Nature of haem-haem interaction. *Nature*, **237**, 495–499.
3. Monod, J., Wyman, J. & Changeux, J.-P. (1965). On the nature of allosteric transitions: a plausible model. *J. Mol. Biol.* **12**, 88–118.
4. Perutz, M. F., Fermi, G., Abraham, D. J., Poyart, C. & Bursaux, E. (1986). Hemoglobin as a receptor of drugs and peptides: X-ray studies of the stereochemistry of binding. *J. Am. Chem. Soc.* **108**, 1064–1078.
5. Arnone, A. (1972). X-ray diffraction study of binding of 2,3-diphosphoglycerate to human deoxyhaemoglobin. *Nature*, **237**, 146–149.
6. Marden, M. C., Bohn, B., Kister, J. & Poyart, C. (1990). Effectors of hemoglobin. Separation of allosteric and affinity factors. *Biophys. J.* **57**, 397–403.
7. Tsuneshige, A., Park, S. & Yonetani, T. (2002). Heterotropic effectors control the hemoglobin function by interacting with its T and R states—A new view on the principle of allostery. *Biophys. Chem.* **98**, 49–63.
8. Shibayama, N., Miura, S., Tame, J. R. H., Yonetani, T. & Park, S. Y. (2002). Crystal structure of horse carbonmonoxyhemoglobin-bezafibrate complex at 1.55-Å resolution. A novel allosteric binding site in R-state hemoglobin. *J. Biol. Chem.* **277**, 38791–38796.
9. Yokoyama, T., Neya, S., Tsuneshige, A., Yonetani, T., Park, S. Y. & Tame, J. R. H. (2006). R-state haemoglobin with low oxygen affinity: crystal structures of deoxy human and carbonmonoxy horse haemoglobin bound to the effector molecule L35. *J. Mol. Biol.* **356**, 790–801.
10. Nagai, K., Perutz, M. F. & Poyart, C. (1985). Oxygen binding properties of human mutant hemoglobins synthesized in *Escherichia coli*. *Proc. Natl Acad. Sci. USA*, **82**, 7252–7255.
11. Nagai, K., Luisi, B., Shih, D., Miyazaki, G., Imai, K.,

- Poyart, C. *et al.* (1987). Distal residues in the oxygen binding site of haemoglobin studied by protein engineering. *Nature*, **329**, 858–860.
12. Olson, J. S., Mathews, A. J., Rohlfs, R. J., Springer, B. A., Egeberg, K. D., Sligar, S. G. *et al.* (1988). The role of the distal histidine in myoglobin and haemoglobin. *Nature*, **336**, 265–266.
 13. Tame, J., Shih, D. T., Pagnier, J., Fermi, G. & Nagai, K. (1991). Functional role of the distal valine (E11) residue of alpha subunits in human haemoglobin. *J. Mol. Biol.* **218**, 761–767.
 14. Mathews, A. J., Rohlfs, R. J., Olson, J. S., Tame, J., Renaud, J. P. & Nagai, K. (1989). The effects of E7 and E11 mutations on the kinetics of ligand binding to R state human hemoglobin. *J. Biol. Chem.* **264**, 16573–16583.
 15. Shaanan, B. (1983). Structure of human oxyhaemoglobin at 2.1 Å resolution. *J. Mol. Biol.* **171**, 31–59.
 16. Lukin, J. A., Simplaceanu, V., Zou, M., Ho, N. T. & Ho, C. (2000). NMR reveals hydrogen bonds between oxygen and distal histidines in oxyhemoglobin. *Proc. Natl Acad. Sci. USA*, **97**, 10354–10358.
 17. Baldwin, J. M. (1980). The structure of human carbonmonoxy haemoglobin at 2.7 Å resolution. *J. Mol. Biol.* **136**, 103–128.
 18. Derewenda, Z., Dodson, G., Emsley, P., Harris, D., Nagai, K., Perutz, M. & Reynaud, J. P. (1990). Stereochemistry of carbon monoxide binding to normal human adult and Cowtown haemoglobins. *J. Mol. Biol.* **211**, 515–519.
 19. Kuriyan, J., Wilz, S., Karplus, M. & Petsko, G. A. (1986). X-ray structure and refinement of carbonmonoxy (Fe II)-myoglobin at 1.5 Å resolution. *J. Mol. Biol.* **192**, 133–154.
 20. Vasquez, G. B., Ji, X., Fronticelli, C. & Gilliland, G. L. (1998). Human carboxyhemoglobin at 2.2 Å resolution: structure and solvent comparisons of R-state, R2-state and T-state hemoglobins. *Acta Crystallog. sect. D*, **54**, 355–366.
 21. Fermi, G., Perutz, M. F., Shaanan, B. & Fourme, R. (1984). The crystal structure of human deoxyhaemoglobin at 1.74 Å resolution. *J. Mol. Biol.* **175**, 159–174.
 22. Tame, J. R. H. & Vallone, B. (2000). The structures of deoxy human haemoglobin and the mutant Hb Tyr α 42His at 120 K. *Acta Crystallog. sect. D*, **56**, 805–811.
 23. Sheldrick, G. M. & Schneider, T. R. (1997). SHELXL: High-resolution refinement. In *Methods in Enzymology* (Sweet, R. M. & Carter, C. W., Jr, eds), vol. 277, pp. 319–343. Academic Press, Orlando.
 24. Srinivasan, R. & Rose, G. D. (1994). The T-to-R transformation in hemoglobin: a reevaluation. *Proc. Natl Acad. Sci. USA*, **91**, 11113–11117.
 25. Schneider, T. R. (2002). A genetic algorithm for the identification of conformationally invariant regions in protein molecules. *Acta Crystallog. sect. D*, **58**, 195–208.
 26. Baldwin, J. & Chothia, C. (1979). Haemoglobin: the structural changes related to ligand binding and its allosteric mechanism. *J. Mol. Biol.* **129**, 175–220.
 27. Yokoyama, T., Chong, K. T., Miyazaki, G., Morimoto, H., Shih, D. T., Unzai, S. *et al.* (2004). Novel mechanisms of pH sensitivity in tuna hemoglobin: a structural explanation of the Root effect. *J. Biol. Chem.* **279**, 28632–28640.
 28. Yonetani, T., Yamamoto, H. & Iizuka, T. (1974). Studies on cobalt myoglobins and hemoglobins III. Electron paramagnetic resonance studies of reversible oxygenation of cobalt myoglobins and hemoglobins. *J. Biol. Chem.* **249**, 2168–2174.
 29. Kachalova, G. S., Popov, A. N. & Bartunik, H. D. (1999). A steric mechanism for inhibition of CO binding to heme proteins. *Science*, **284**, 473–476.
 30. Sigfridsson, E. & Ryde, U. (2002). Theoretical study of the discrimination between O(2) and CO by myoglobin. *J. Inorg. Biochem.* **91**, 101–115.
 31. Vojtechovsky, J., Chu, K., Berendzen, J., Sweet, R. M. & Schlichting, I. (1999). Crystal structures of myoglobin-ligand complexes at near-atomic resolution. *Biophys. J.* **77**, 2153–2174.
 32. Perutz, M. F. (1968). Preparation of haemoglobin crystals. *J. Cryst. Growth*, **2**, 54–56.
 33. Juers, D. H. & Matthews, B. W. (2001). Reversible lattice packing illustrates the temperature dependence of macromolecular interactions. *J. Mol. Biol.* **311**, 851–862.
 34. Juers, D. H. & Matthews, B. W. (2004). Cryo-cooling in macromolecular crystallography: advantages, disadvantages and optimization. *Quart. Rev. Biophys.* **37**, 105–119.
 35. van't Hoff, J. H. (1884). Etudes de dynamique chimique.
 36. Baldwin, R. B. (1986). Temperature dependence of the hydrophobic interaction in protein folding. *Proc. Natl Acad. Sci. USA*, **83**, 8069–8072.
 37. Kumar, S., Tsai, C.-J. & Nussinov, R. (2000). Factors enhancing protein thermostability. *Protein Eng.* **13**, 179–191.
 38. Ward, K. B., Wishner, B. C., Lattman, E. E. & Love, W. E. (1975). Structure of deoxyhemoglobin A crystals grown from polyethylene glycol solutions. *J. Mol. Biol.* **98**, 161–177.
 39. Paoli, M., Liddington, R., Tame, J., Wilkinson, A. & Dodson, G. (1996). Crystal structure of T state haemoglobin with oxygen bound at all four haems. *J. Mol. Biol.* **256**, 775–792.
 40. Paoli, M., Dodson, G., Liddington, R. C. & Wilkinson, A. J. (1997). Tension in haemoglobin revealed by Fe-His(F8) bond rupture in the fully liganded T-state. *J. Mol. Biol.* **271**, 161–167.
 41. Silva, M. M., Rogers, P. H. & Arnone, A. (1992). A third quaternary structure of human hemoglobin A at 1.7-Å resolution. *J. Biol. Chem.* **267**, 17248–172456.
 42. Mueser, T. C., Rogers, P. H. & Arnone, A. (2000). Interface sliding as illustrated by the multiple quaternary structures of liganded hemoglobin. *Biochemistry*, **39**, 15353–15364.
 43. Xu, C., Tobi, D. & Bahar, I. (2003). Allosteric changes in protein structure computed by a simple mechanical model: hemoglobin T \leftrightarrow R2 transition. *J. Mol. Biol.* **333**, 153–168.
 44. Perutz, M. F., Wilkinson, A. J., Paoli, M. & Dodson, G. G. (1998). The stereochemical mechanism of the cooperative effects in hemoglobin revisited. *Annu. Rev. Biophys. Biomol. Struct.* **27**, 1–34.
 45. Lukin, J. A., Kontaxis, G., Simplaceanu, V., Yuan, Y., Bax, A. & Ho, C. (2003). Quaternary structure of hemoglobin in solution. *Proc. Natl Acad. Sci. USA*, **100**, 517–520.
 46. Lukin, J. A. & Ho, C. (2004). The structure-function relationship of hemoglobin in solution at atomic resolution. *Chem. Rev.* **104**, 1219–1230.
 47. Tame, J. R. H. (1999). What is the true structure of liganded haemoglobin? *Trends Biochem. Sci.* **24**, 372–377.
 48. Rujan, I. N. & Russu, I. M. (2002). Allosteric effects of chloride ions at the intradimeric α 1 β 1 and α 2 β 2 interfaces of human hemoglobin. *Proteins; Struct. Funct. Genet.* **49**, 413–419.
 49. Kavanaugh, J. S., Rogers, P. H. & Arnone, A. (2005). Crystallographic evidence for a new ensemble of ligand-induced allosteric transitions in hemoglobin: the T-to-T(high) quaternary transitions. *Biochemistry*, **44**, 6101–6121.

50. Samuni, U., Juszczak, L., Dantsker, D., Khan, I., Friedman, A. J., Perez-Gonzalez-de-Apodaca, J. *et al.* (2003). Functional and spectroscopic characterization of half-liganded iron-zinc hybrid hemoglobin: evidence for conformational plasticity within the T state. *Biochemistry*, **42**, 8272–8288.
51. Luisi, B., Liddington, B., Fermi, G. & Shibayama, N. (1990). Structure of deoxy-quaternary haemoglobin with liganded beta subunits. *J. Mol. Biol.* **214**, 7–14.
52. Luisi, B. & Shibayama, N. (1989). Structure of haemoglobin in the deoxy quaternary state with ligand bound at the alpha haems. *J. Mol. Biol.* **206**, 723–736.
53. Morris, R. J., Neckameyer, W. S. & Gibson, Q. H. (1981). Multiple T state conformations in a fish hemoglobin. Carbon monoxide binding to hemoglobin of *Thunnus thynnus*. *J. Biol. Chem.* **256**, 4598–4603.
54. Miyazaki, G., Morimoto, H., Yun, K. M., Park, S. Y., Nakagawa, A., Minagawa, H. & Shibayama, N. (1999). Magnesium(II) and zinc(II)-protoporphyrin IX's stabilize the lowest oxygen affinity state of human hemoglobin even more strongly than deoxy-heme. *J. Mol. Biol.* **292**, 1121–1136.
55. Park, S. Y., Shibayama, N., Hiraki, T. & Tame, J. R. H. (2004). Crystal structures of unliganded and half-liganded human hemoglobin derivatives cross-linked between Lys 82beta1 and Lys 82beta2. *Biochemistry*, **43**, 8711–8717.
56. Ho, C. (1992). Proton nuclear magnetic resonance studies on hemoglobin: cooperative interactions and partially ligated intermediates. *Adv. Protein Chem.* **43**, 153–312.
57. Gong, Q., Simplaceanu, V., Lukin, J. A., Giovannelli, J. L., Ho, N. T. & Ho, C. (2006). Quaternary structure of carbonmonoxyhemoglobins in solution: structural changes induced by the allosteric effector inositol hexaphosphate. *Biochemistry*, **45**, 5140–5148.
58. Yonetani, T., Park, S. I., Tsuneshige, A., Imai, K. & Kanaori, K. (2002). Global allostery model of hemoglobin. Modulation of O(2) affinity, cooperativity, and Bohr effect by heterotropic allosteric effectors. *J. Biol. Chem.* **277**, 34508–34520.
59. Safo, M. K., Burnett, J. C., Musayev, F. N., Nokuri, S. & Abraham, D. J. (2002). Structure of human carbonmonoxyhemoglobin at 2.16 Å: a snapshot of the allosteric transition. *Acta Crystallog. sect. D*, **58**, 2031–2037.
60. Wilson, J., Phillips, K. & Luisi, B. (1996). The crystal structure of horse deoxyhaemoglobin trapped in the high-affinity (R) state. *J. Mol. Biol.* **264**, 743–756.
61. Schumacher, M. A., Dixon, M. M., Kluger, R., Jones, R. T. & Brennan, R. G. (1995). Allosteric transition intermediates modelled by crosslinked haemoglobins. *Nature*, **375**, 84–87.
62. Safo, M. K. & Abraham, D. J. (2005). The enigma of the liganded hemoglobin end state: a novel quaternary structure of human carbonmonoxy hemoglobin. *Biochemistry*, **44**, 8347–8359.
63. Imai, K. (1982). *Allosteric Effects in Haemoglobin*, Cambridge University Press, Cambridge.
64. Yonetani, T. & Tsuneshige, A. (2003). The global allostery model of hemoglobin: an allosteric mechanism involving homotropic and heterotropic interactions. *C.R. Biol.* **326**, 523–532.
65. Leslie, A. G. W. (1992). Recent changes to the MOSFLM package for processing film and image plate data. *Joint CCP4 + ESF-EAMCB Newsletter on Protein Crystallography*, **26**.
66. CCP4 (1994). The CCP4 suite: programs for protein crystallography. *Acta Crystallog. sect. D*, **50**, 760–763.
67. Otwinowski, Z. & Minor, W. (1997). Processing of X-ray diffraction data collected in oscillation mode. *Methods Enzymol.* **276**, 307–326.
68. Brunger, A. T. (1996). *X-PLOR v 3.851*. Yale University, New Haven.
69. Roussel, A. & Cambillau, C. (1989). *Silicon Graphics Geometry Partner Directory*, pp. 77–78. Silicon Graphics, Mountain View, CA.
70. Emsley, P. & Cowtan, K. (2004). COOT: model-building tools for molecular graphics. *Acta Crystallog. sect. D*, **60**, 2126–2132.

Edited by R. Huber

(Received 3 March 2006; received in revised form 8 May 2006; accepted 16 May 2006)
Available online 30 May 2006